

## Validation of a multicolor staining to monitor $\text{phosphoSTAT5}$ levels in regulatory T-cell subsets

Grégory Ehx<sup>1,\*</sup>, Muriel Hannon<sup>1,\*</sup>, Yves Beguin<sup>1,2</sup>, Stéphanie Humblet-Baron<sup>1,3,\*\*</sup> and Frédéric Baron<sup>1,2,\*\*</sup>

<sup>1</sup> Hematology Research Unit, Groupe Interdisciplinaire de Génoprotéomique Appliquée (GIGA)-I<sup>3</sup>, University of Liège, Liège, Belgium

<sup>2</sup> Department of Medicine, Division of Hematology, CHU of Liège, Liège, Belgium

<sup>3</sup> Autoimmune Genetics Laboratory, University of Leuven, Leuven, Belgium

\* These authors are co-first authors

\*\* These authors are co-senior authors

Correspondence to: Grégory Ehx, email: g.ehx@ulg.ac.be

Keywords: Treg, regulatory T cells, FOXP3, STAT5, IL-2, Immunology and Microbiology Section, Immune response, Immunity

Received: September 14, 2015

Accepted: November 26, 2015

Published: December 07, 2015

### ABSTRACT

**BACKGROUND:** Regulatory T cells ( $T_{\text{regs}}$ ) are key players in immune tolerance. They express the transcription factor FOXP3 and are dependent of the STAT5 signaling for their homeostasis. So far, the study of phosphorylated epitopes by flow cytometry required treating the cells with methanol, which is harmful for several epitopes.

**METHODS:** Here we assessed whether the PerFix EXPOSE reagent kit (PFE) (Beckman Coulter) allowed monitoring the phosphorylation level of STAT5 in  $T_{\text{reg}}$  subpopulations together with complex immunophenotyping. Results observed with the PFE kit were compared to those observed without cell permeabilization for surface markers, with paraformaldehyde permeabilization for non-phosphorylated intracellular epitopes, and with methanol-based permeabilization for  $\text{phosphoSTAT5}$  staining.

**RESULTS:** In human PBMCs, the PFE kit allowed the detection of surface antigens, FOXP3, KI67 and  $\text{phosphoSTAT5}$  in similar proportions to what was observed without permeabilization (for surface antigens), or with PFA or methanol permeabilizations for FOXP3/KI67 and  $\text{phosphoSTAT5}$ , respectively. Comparable observations were made with murine splenocytes. Further, the PFE kit allowed determining the response of different human and murine  $T_{\text{reg}}$  subsets to IL-2. It also allowed demonstrating that human  $T_{\text{reg}}$  subsets with the highest levels of  $\text{phosphoSTAT5}$  had also the highest suppressive activity *in vitro*, and that anti-thymocyte globulin (ATG) induced  $T_{\text{reg}}$  independently of the STAT5 pathway, both *in vitro* and *in vivo*.

**CONCLUSIONS:** We have validated a multicolor staining method that allows monitoring  $\text{phosphoSTAT5}$  levels in  $T_{\text{reg}}$  subsets. This staining could be useful to monitor responses of various  $T_{\text{reg}}$  subsets to IL-2 therapy.

### INTRODUCTION

Regulatory T cells ( $T_{\text{regs}}$ ) represent a fraction of  $CD4^+$  T cells that are indispensable for maintaining immunological self tolerance [1, 2]. They express the forkhead box protein 3 factor (FOXP3) in their nuclei, and CD25 (the high-affinity component of the trimeric form of the interleukin 2 (IL-2) receptor) on their cell surface [3,

4].  $T_{\text{regs}}$  are also featured by a low expression of CD127, the  $\alpha$  chain of the IL-7 receptor [5].

The main population of  $T_{\text{regs}}$  is generated in the thymus, where high-avidity recognition of self-antigens by their T-cell receptor (TCR) leads to the generation of thymus  $T_{\text{regs}}$  [6, 7]. However,  $T_{\text{regs}}$  can also be generated in the periphery (peripheral  $T_{\text{regs}}$ ) from conversion from conventional  $CD4^+$  T cells ( $T_{\text{convs}}$ ), or *in vitro* from

naive  $T_{conv}$  by TCR stimulation along with TGF- $\beta$ , IL-10 or retinoic acid signaling (induced  $T_{regs}$ ) [6]. In addition to distinctions based on their origin,  $T_{reg}$  can be further subdivided into central or naive  $T_{regs}$  (that are CD45RA<sup>+</sup>CCR7<sup>+</sup> in humans and CD62L<sup>hi</sup>CCR7<sup>+</sup> in mice), and effector  $T_{regs}$  (that are CD45RA<sup>neg</sup> in humans, and CD62L<sup>low</sup>CCR7<sup>low</sup>CD44<sup>high</sup> and CD103<sup>+</sup> in mice) [4, 7-9]. Importantly, in humans, effector  $T_{regs}$  can be further separated between activated (HLA-DR<sup>+</sup>) effector  $T_{regs}$  that are highly proliferating, and HLA-DR<sup>neg</sup> effector  $T_{regs}$  that are less proliferating [9].

In the last decade, animal studies have evidenced that restoring the T-cell balance in favor of  $T_{regs}$  allowed the control of autoimmunity in several animal models of rheumatologic diseases [10]. Further,  $T_{reg}$  administration prevented graft-versus-host disease (GVHD, a redoubtable complication of allogeneic hematopoietic cell transplantation caused by donor immune cells contained in the graft reacting against recipient healthy tissues [11]) both in mouse to mouse and in humanized mouse models of GVHD [12-15]. Further,  $T_{reg}$  infusion also prolonged human skin graft survival in humanized mice [16].

These observations in animal models prompted the initiation of pilot clinical studies of  $T_{reg}$  infusion as prevention or treatment of GVHD [17-19], or as prevention of solid organ rejection [20].

IL-2 is a member of the common cytokine gamma chain family that plays a central role in  $T_{reg}$  homeostasis through stimulation of the STAT5 pathway [4, 21]. This prompted Koreth *et al.* to investigate the safety and efficacy of low-dose IL-2 administration (with the aim of boosting  $T_{regs}$ ) in patients with chronic GVHD [22]. The authors observed that administration of low-dose IL-2 not only successfully increased  $T_{reg}$  blood counts but also induced clinical responses in half of the patients. Administration of low-dose IL-2 resulted also in increased  $T_{reg}$  counts and clinical responses in patients with autoimmune diseases such as hepatitis C virus-induced vasculitis [23] or type 1 diabetes [24]. With the development of such cytokine-based immunotherapies, monitoring of the phosphorylation level of key players in target signaling pathways (and particularly of STAT5), simultaneously in several cell sub-populations, is of great interest in order to assess treatment efficacy early.

So far, the study of phosphorylated epitopes by flow cytometry required treating the cells with methanol, which is harmful for many extra- and intra-cellular epitopes and compromises multiparameter analyses. Recently, a new reagent kit, the PerFix EXPOSE kit (Beckman Coulter), was designed to allow studying phosphorylated epitopes without compromising other epitopes. In the present report, we compared this new procedure with reference permeabilization protocols for (non)-phosphorylated epitopes to validate it and used it to study  $T_{reg}$  subsets response to IL-2 in human and mouse samples. Our results showed that the PerFix technique is suitable for combined

$T_{reg}$  STAT5 monitoring and accurate immunophenotyping in human and mouse samples. We also highlighted differential responses to IL-2 among  $T_{reg}$  subsets.

## RESULTS AND DISCUSSION

### Validation of a multicolor staining to monitor phospho-STAT5 levels in human $T_{reg}$ subsets

To assess the capacity of the PFE kit to allow the accurate quantification of phospho-STAT5 in combination with surface (CD4, CD25, CD127, HLA-DR and CD45RA) and non-phosphorylated intracellular (FOXP3, KI67) epitopes, we compared this procedure with the conventional permeabilization method for phospho-epitopes (Methanol (MeOH)-based method) and the conventional permeabilization procedure for FOXP3 and KI67 staining (Paraformaldehyde (PFA) -based method). In order to assess the impact of any permeabilization treatment on the expression of surface epitopes, cells were also analyzed after staining of surface epitopes without any further permeabilization. These comparisons were repeated twice with 8 healthy volunteers and similar results were found in each experiment. Results from the first experiment are presented hereafter as representative example. The following combination of antibodies was used: CD4-PE-Cy5, CD25-BV421, CD127-biotin-streptavidin-PE-Cy7, CD45RA-BV510, HLA-DR-APC-efluor780, FOXP3-AlexaFluor488, KI67-PE and phospho-STAT5-AlexaFluor647 (detailed in materials and methods).

Using the gating strategy described in Figure 1A, we observed similar frequencies of CD4<sup>+</sup>, CD25<sup>high</sup>CD127<sup>low</sup> and CD25<sup>low/int</sup>CD127<sup>high</sup> cells among non-permeabilized cells, and cells permeabilized with either the PFE, PFA or MeOH methods (Figure 1B-1D).

Next we compared FOXP3<sup>+</sup> frequency within the CD25<sup>high</sup>CD127<sup>low</sup> population and observed comparable FOXP3<sup>+</sup> frequency among cells permeabilized with the PFA or with the PFE method, highlighting the successful and accurate staining of FOXP3 with this later procedure (Figure 1E). In contrast, there was a trend for decreased FOXP3<sup>+</sup> frequency within the CD4<sup>+</sup>CD25<sup>high</sup>CD127<sup>low</sup> population in cells permeabilized with the MeOH procedure. Regarding KI67 staining, no significant difference of frequency within either  $T_{reg}$  or  $T_{conv}$  populations was found between the three permeabilization protocols (Figure 1F).

Importantly, similar proportions of naive and activated effector  $T_{regs}$  were observed with the PFA and PFE procedures (Figure 1G-1H). In contrast, the methanol permeabilization procedure strikingly decreased the frequency of naive  $T_{regs}$ , highlighting the deleterious impact of this permeabilization technique on certain

surface epitopes such as CD45RA, although we can not exclude that by trying several CD45RA epitopes satisfying results could have been achieved also with the methanol technique.

Next, we compared STAT5 phosphorylation levels (evaluated as mean fluorescence intensity (MFI) of  $\text{phospho-STAT5-APC}$ ) in  $T_{\text{regs}}$  normalized on  $T_{\text{conv}}$   $\text{phospho-STAT5}$  levels to reduce inter-assay variability of MFI between PFE and methanol permeabilization methods, after stimulation with 10 IU/ml of IL-2. Importantly, no difference between the two methods was observed (Figure 1I), demonstrating the reliability of the PFE technique for  $\text{phospho-STAT5}$  analysis. This experiment further evidenced higher levels of  $\text{phospho-STAT5}$  in  $T_{\text{regs}}$  than in  $T_{\text{conv}}$  following stimulation with low-dose IL-2, as recently observed by another group of investigators [24].

Finally, we assessed the variability for each

donor between the PFE and reference technique (PFA or MeOH). Using simple linear regressions, we found a strong positive correlation (Spearman  $r \geq 0.88$ ,  $p \leq 0.0072$ ) between the results of the PFE and reference method for  $CD4^+$ ,  $CD25^{\text{high}}CD127^{\text{low}}$ ,  $CD25^{\text{low/int}}CD127^{\text{high}}$  ( $T_{\text{conv}}$ ),  $CD45RA^+ T_{\text{reg}}$ ,  $HLA-DR^+ T_{\text{reg}}$  and  $T_{\text{reg}}/T_{\text{conv}}$   $\text{phospho-STAT5}$  ratio (Supplemental Figure 1). In contrast, there was no correlation for FOXP3<sup>+</sup> and KI67<sup>+</sup> cells frequency within  $CD25^{\text{high}}CD127^{\text{low}}$  and  $T_{\text{regs}}$  respectively, likely because of the low inter-donor variability of these parameters. However, importantly, there was a significant correlation for the frequency of  $CD25^{\text{high}}CD127^{\text{low}}FOXP3^+$  cells ( $T_{\text{regs}}$ ) among total lymphocytes ( $r = 0.83$ ,  $p = 0.0184$ ) or  $CD4^+$  T cells ( $r = 0.97$ ,  $p = 0.0004$ ), as well as for the frequencies of the different  $T_{\text{reg}}$  subpopulations among  $CD4^+$  T cells (naive Treg:  $r = 0.88$ ,  $p = 0.0072$ ; effector Treg:  $r = 0.97$ ,  $p = 0.0004$ ; and activated effector Treg:  $r = 0.76$ ,  $p =$

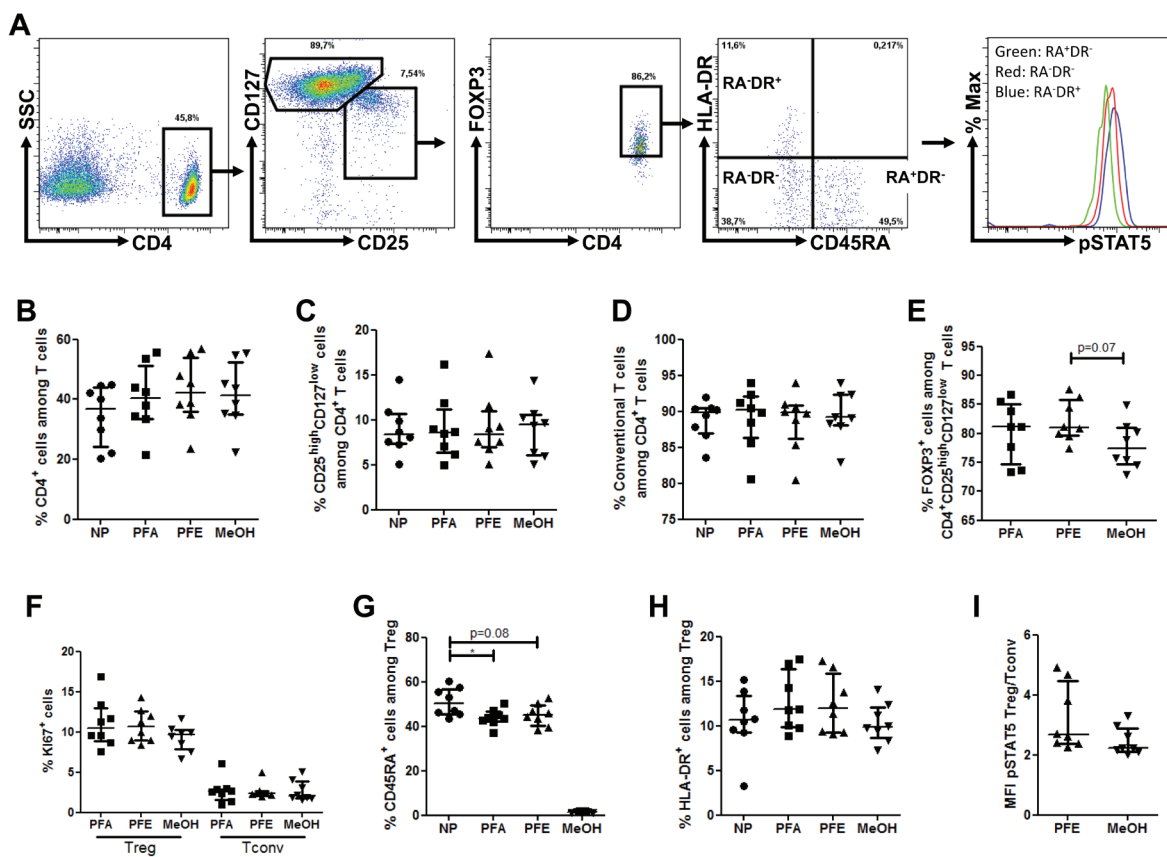


**Figure 1: PerFix EXPOSE allows accurate detection of  $\text{phospho-STAT5}$  together with surface and intracellular immunophenotyping.** PBMC from 8 healthy volunteers were surface stained with anti-CD4, -CD25, -CD127, -CD45RA and -HLA-DR antibodies and were either non permeabilized (NP) or stained with anti-FOXP3, -KI67 and  $\text{phospho-STAT5}$  antibodies after permeabilization with either paraformaldehyde (PFA)-based technique, PerFix EXPOSE (PFE) or methanol (MeOH)-based technique. Data show median values of 8 biological replicates / condition with interquartile range (\*  $p < 0.05$ , \*\*  $p < 0.005$ , \*\*\*  $p < 0.0005$ ). **A.** Gating strategy of tubes permeabilized with the PerFix method. **B.-H.** Comparison of cell frequencies between the different permeabilization methods:  $CD4^+$  T-cell frequency among the total lymphocyte population **B.**,  $CD25^{\text{high}}CD127^{\text{low}}$  among  $CD4^+$  T cells **C.**,  $T_{\text{conv}}$  ( $CD25^{\text{low/int}}CD127^{\text{high}}$ ) among  $CD4^+$  T cells **D.**, FOXP3<sup>+</sup> among  $CD25^{\text{high}}CD127^{\text{low}}$  cells **E.**, KI67<sup>+</sup> cell frequency among either  $T_{\text{reg}}$  or  $T_{\text{conv}}$  populations **F.**,  $CD45RA^+$  among  $CD4^+CD25^{\text{high}}CD127^{\text{low}}FOXP3^+$   $T_{\text{reg}}$  **G.** and HLA-DR<sup>+</sup> among  $CD4^+CD25^{\text{high}}CD127^{\text{low}}FOXP3^+$   $T_{\text{reg}}$  **H.** **I.** Comparison of ratio, for each sample, of  $\text{phospho-STAT5}$  MFI of  $T_{\text{regs}}$  versus  $\text{phospho-STAT5}$  MFI of  $T_{\text{conv}}$  in PerFix and methanol-based methods.

0.0368).

Altogether these data validate an 8-color staining method allowing measurement of  $\text{pSTAT5}$  levels in human  $T_{\text{reg}}$  subsets.

### In human PBMCs, activated effector $T_{\text{regs}}$ have higher $\text{pSTAT5}$ levels than other $T_{\text{reg}}$ subsets after stimulation with IL-2

Despite the growing knowledge on human  $T_{\text{regs}}$ , little is known about the homeostatic properties of their sub-populations. Therefore, we took advantage of the PFE kit to study the respective capacities of the different  $T_{\text{reg}}$

subsets at phosphorylating STAT5 in response to IL-2.

First we performed this comparison with low-dose (10 IU/ml) IL-2. The highest  $\text{pSTAT5}$  levels were found in activated effector  $T_{\text{regs}}$ , followed by HLA-DR<sup>neg</sup> effector  $T_{\text{regs}}$ , while naive  $T_{\text{regs}}$  had the lowest levels of  $\text{pSTAT5}$  (Figure 2A). We then examined whether  $\text{pSTAT5}$  levels correlated with CD25 expression by  $T_{\text{regs}}$ . We first observed that, as seen with  $\text{pSTAT5}$  levels, activated effector  $T_{\text{regs}}$  had the highest expression of CD25, followed by HLA-DR<sup>neg</sup> effector  $T_{\text{reg}}$  and naive  $T_{\text{reg}}$  (Figure 2B). These data are in concordance with those reported by Miyara *et al.* showing higher CD25 expression in activated effector  $T_{\text{regs}}$  than in naive  $T_{\text{regs}}$  [8]. Further,

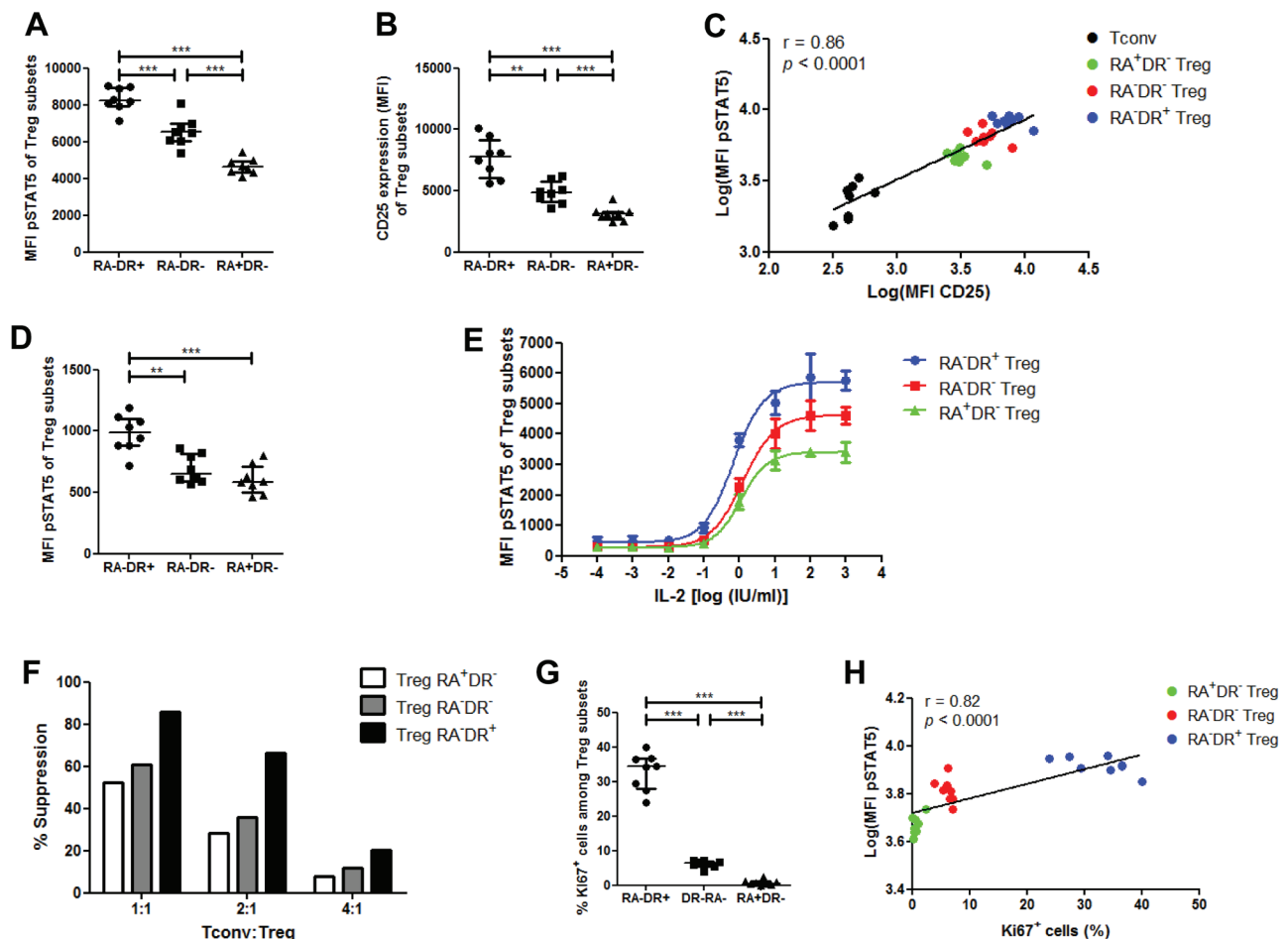


**Figure 2: Phospho-STAT5 comparison between human  $T_{\text{reg}}$  subsets.** A.-C., G.-H. PBMC from 8 healthy volunteers were stimulated with 10 IU/ml of recombinant human IL-2, stained with anti-CD4, -CD25, -CD127, -CD45RA and -HLA-DR antibodies, permeabilized with the PerFix EXPOSE method and stained with anti-FoxP3, -KI67 and - $\text{pSTAT5}$  antibodies. **A.** Comparison of STAT5 phosphorylation level (MFI) between the different  $T_{\text{reg}}$  subsets with IL-2 stimulation, based on their expression of CD45RA and HLA-DR. **B.** CD25 expression (MFI) of the different  $T_{\text{reg}}$  subsets. **C.** Correlation between STAT5 phosphorylation level (log of MFI) and CD25 expression (log of MFI) in  $T_{\text{convs}}$  and the different  $T_{\text{reg}}$  subsets. **D.** Comparison of  $\text{pSTAT5}$  MFI between the different  $T_{\text{reg}}$  subsets without IL-2 stimulation. **E.** Total  $T$  cells were isolated from 3 healthy volunteers, stimulated with various concentrations of IL-2 for 15 min and  $\text{pSTAT5}$  level was measured in the different  $T_{\text{reg}}$  subsets after PerFix EXPOSE permeabilization. Data show mean values with standard deviation. **F.** Comparison of *in vitro* suppressive activity between the different human  $T_{\text{reg}}$  subsets at different  $T_{\text{reg}}:T_{\text{conv}}$  ratios. Data show mean value of triplicates. **G.** Comparison of  $\text{KI67}^+$  cell frequency among the different  $T_{\text{reg}}$  subsets. **H.** Correlation between STAT5 phosphorylation level after stimulation with 10 IU/ml of IL-2 (log of MFI) and  $\text{KI67}^+$  cell frequency in the different  $T_{\text{reg}}$  subsets. Data show median values with interquartile range (\*  $p < 0.05$ , \*\*  $p < 0.005$ , \*\*\*  $p < 0.0005$ ).



taking data from  $T_{conv}$  and  $T_{reg}$  subsets together, there was a strong correlation between  $STAT5^{phospho}$  and CD25 levels (Spearman  $r = 0.86$ ,  $p < 0.0001$ , Figure 2C). These findings demonstrate that the different  $T_{reg}$  subsets are not homogeneous in terms of response to IL-2 stimulation.

In order to verify that these observations remained present in basal conditions, we performed the same analyses with unstimulated  $T_{regs}$  and observed significantly higher  $STAT5^{phospho}$  levels in activated effector  $T_{regs}$  than in the two other  $T_{reg}$  subpopulations, while no differences were detected between HLA-DR<sup>neg</sup> effector  $T_{regs}$  and naive  $T_{regs}$  (Figure 2D).

To further evaluate the response of the various  $T_{reg}$  subsets to IL-2, we compared  $STAT5^{phospho}$  levels in the three  $T_{reg}$  subsets after stimulation with an 8-log range of IL-2 concentration (Figure 2E and Supplemental Figure 2). As observed above, activated effector  $T_{regs}$  had

the highest  $STAT5^{phospho}$  levels, followed by HLA-DR<sup>neg</sup> effector  $T_{regs}$  and naive  $T_{regs}$ . Specifically, the log half maximal effective concentration ( $\log(EC_{50})$ ) of activated effector  $T_{regs}$  (-0.165) was lower than the  $\log(EC_{50})$  of HLA-DR<sup>neg</sup> effector  $T_{regs}$  (0.096,  $p = 0.0495$ ) and naive  $T_{regs}$  (0.039,  $p = 0.0768$ ) subsets, supporting a higher proliferative capacity of this  $T_{reg}$  subset over the two others. These results are consistent with the differences observed in unstimulated  $T_{regs}$  and further demonstrate the heterogeneity of  $T_{reg}$  subsets in terms of response to IL-2 stimulation. In addition, our observations are in line with a recent study reporting that high-dose IL-2 therapy in melanoma patients promoted a  $T_{reg}$  subset with an activated phenotype [25]. Interestingly, we observed that the activated effector  $T_{regs}$  had the highest suppressive activity *in vitro*, while the two other populations presented similar (lower) suppressive activities (Figure 2F). These

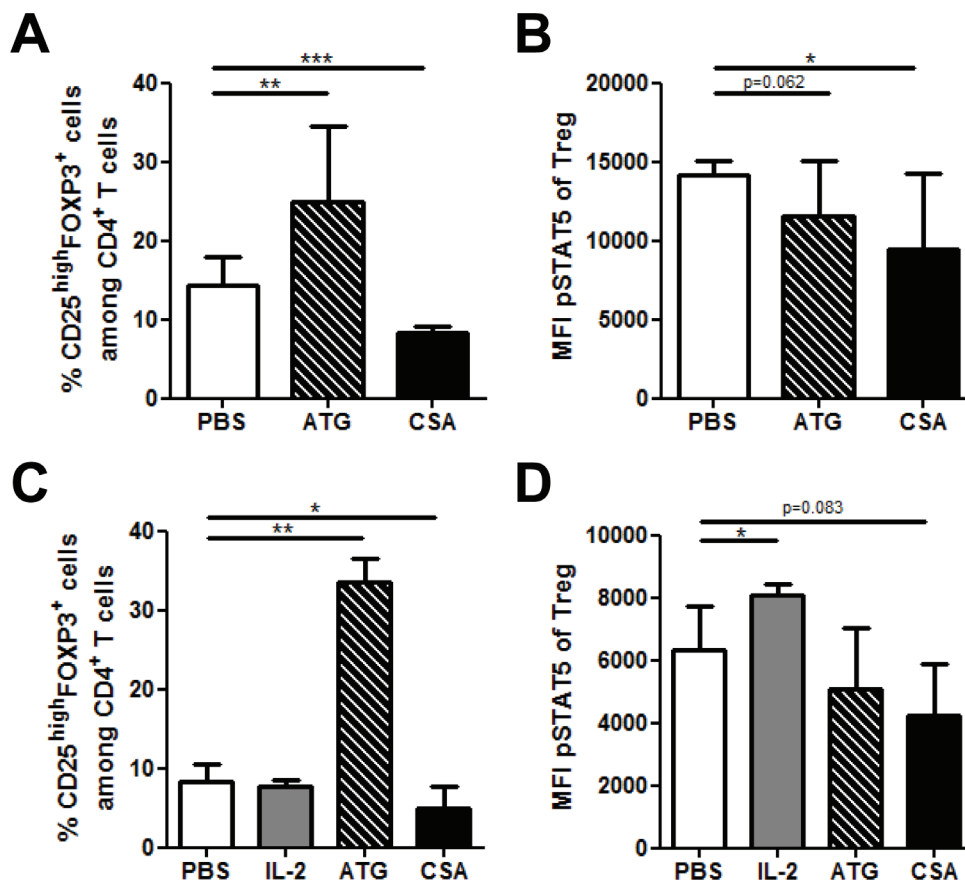


**Figure 3: Impact of Anti-thymocyte globulin (ATG) and cyclosporin A (CSA) on  $T_{reg}$   $STAT5^{phospho}$  levels *in vivo* and *in vitro*.** A.-B. Human PBMCs, freshly isolated from 3 healthy donors were cultured in triplicate in the presence of either PBS, CSA (500 ng/ml) or ATG (100  $\mu$ g/ml) for 24 hours. The impact of these compounds on CD4<sup>+</sup>CD25<sup>high</sup>FOXP3<sup>+</sup> cell frequency A. as well as on  $STAT5^{phospho}$  levels in  $T_{regs}$  B. was assessed by flow cytometry using the PFE technique for permeabilization. Data show median values of 9 replicates (3 biological replicates in triplicates / condition) with interquartile range (\*  $p < 0.05$ , \*\*  $p < 0.005$ , \*\*\*  $p < 0.0005$ ). (C-D) NSG mice received 2.5 Gy total body irradiation and were injected with  $5 \times 10^6$  human PBMC *i.v.* 24h later (day 0). They were injected with either PBS (daily from day 4 to 6), 15 mg/kg of cyclosporin A (CSA, daily from day 4 to 6), 10 mg/kg of ATG (day 6) or 50.000 IU of IL-2 (24h, 12h and 1h before sacrifice). At day 7, animals were sacrificed and spleens were collected for flow cytometry comparison of CD4<sup>+</sup>CD25<sup>high</sup>FOXP3<sup>+</sup> cells frequency A. and  $STAT5^{phospho}$  level in  $T_{regs}$  B. between the different treatments (PFE technique was used for permeabilization). Data show median values of 8 biological replicates with interquartile range (\*  $p < 0.05$ , \*\*  $p < 0.005$ , \*\*\*  $p < 0.0005$ ).

results suggest that  $\text{STAT5}^{\text{phospho}}$  level of  $T_{\text{reg}}$  subsets might be predictive of their suppressive function.

Finally, we compared KI67 expression between  $T_{\text{reg}}$  subsets and found the highest frequency of KI67<sup>+</sup> cells within the activated effector  $T_{\text{reg}}$  fraction, while the HLA-DR<sup>neg</sup> effector  $T_{\text{regs}}$  had a higher KI67 expression than naive  $T_{\text{regs}}$  (Figure 2G), in agreement with previous findings [9]. Given the pivotal function of STAT5 phosphorylation in  $T_{\text{reg}}$  proliferation, a significant correlation was found between KI67 expression of  $T_{\text{reg}}$  subsets and their level of  $\text{STAT5}^{\text{phospho}}$  after low-dose IL-2 stimulation (Spearman  $r = 0.82$ ,  $p < 0.0001$ , Figure 2H).

Because cryopreserved rather than fresh PBMCs are frequently used in clinical trials, we assessed  $\text{STAT5}^{\text{phospho}}$  levels in  $T_{\text{reg}}$  subsets recovered from human cryopreserved PBMCs. As observed with freshly isolated PBMCs, activated effector  $T_{\text{regs}}$  from cryopreserved PBMCs presented the highest levels of  $\text{STAT5}^{\text{phospho}}$ , CD25 and KI67 in comparison with the two other subsets, while effector  $T_{\text{regs}}$  had significantly higher levels of these markers than naive  $T_{\text{regs}}$  (Supplemental Figure 3). These data indicate that the PFE technique is reliable also for thawed PBMC samples.

Altogether these data suggest that the different proliferative capacities of  $T_{\text{reg}}$  subsets may be dependent upon their divergent capacities to respond to IL-2 through the STAT5 pathway.

### Impact of anti-thymocyte globulin (ATG) and cyclosporin A on $T_{\text{reg}} \text{STAT5}^{\text{phospho}}$ levels

Immunosuppressive drugs, such as anti-thymocyte globulin (ATG) and cyclosporin A (CSA) are widely used to prevent or treat pathologies where  $T_{\text{conv}}$  and  $T_{\text{regs}}$  play a critical role such as GVHD [26]. To gain further insight on the impact of these drugs on  $T_{\text{regs}}$ , we assessed their impact on  $\text{STAT5}^{\text{phospho}}$  levels using the PFE technique. We first assessed this impact *in vitro* and observed that ATG dramatically increased the frequency of CD4<sup>+</sup>CD25<sup>high</sup>FOXP3<sup>+</sup>  $T_{\text{regs}}$  (as observed previously by other investigators [27, 28]), while  $T_{\text{reg}}$  frequency was reduced by CSA (Figure 3A). Interestingly, both ATG and CSA significantly reduced  $\text{STAT5}^{\text{phospho}}$  levels in  $T_{\text{regs}}$  (Figure 3B). This suggests that  $T_{\text{reg}}$  expansion by ATG is independent of STAT5 signaling and is rather the result of the conversion of  $T_{\text{conv}}$  into  $T_{\text{regs}}$ , as previously showed by other investigators [27]. In addition, the lowered levels of  $\text{STAT5}^{\text{phospho}}$  by CSA are probably the results of its inhibitory effect on IL-2 production.

We next investigated the impact of these compounds *in vivo* in NSG mice transplanted with human PBMCs. We observed that, in agreement with *in vitro* experiments, ATG dramatically increased  $T_{\text{reg}}$  frequency, while the opposite was observed with CSA (Figure 3C). Further, while IL-2 significantly increased  $\text{STAT5}^{\text{phospho}}$  levels

in  $T_{\text{regs}}$ , the opposite was observed with ATG and CSA (Figure 3D).

### Validation of a multicolor staining to monitor $\text{STAT5}^{\text{phospho}}$ levels in mouse $T_{\text{reg}}$

We next assessed the capacity of the PFE kit to allow the accurate quantification of  $\text{STAT5}^{\text{phospho}}$  levels in combination with surface (CD3, CD4, CD8, CD25) and non-phosphorylated intracellular (FOXP3 and Ki67) epitopes in murine splenocytes from 5 B10.D2 and 5 B10.BR mice (Figure 4A). The following combination of antibodies was used: CD3-V500, CD4-eFluor450, CD8-PE-Cy7, CD25-PerCP-Cy5.5, FoxP3-PE, Ki67-FITC and  $\text{STAT5}^{\text{phospho}}$ -AlexaFluor647 (detailed in material and methods).

In slight contrast to what was observed with human PBMCs, the PFE kit slightly reduced the expression (MFI) of both CD25 and FoxP3 by  $T_{\text{regs}}$ , while no impact was observed on CD3, CD4 and CD8 staining (Figure 4B). However, importantly, the frequencies of CD3<sup>+</sup>, CD3<sup>+</sup>CD4<sup>+</sup>, CD3<sup>+</sup>CD8<sup>+</sup>, and CD3<sup>+</sup>CD4<sup>+</sup>CD25<sup>+</sup>FoxP3<sup>+</sup> lymphocytes were similar between PFE and either not permeabilized or PFA samples (Figure 4C). Further, the percentage of cells expressing the proliferation marker Ki67 was also comparable with the PFA and PFE kits (Figure 4D). In contrast, methanol-based permeabilization resulted in an almost complete loss of CD25 staining hampering proper gating of CD3<sup>+</sup>CD4<sup>+</sup>CD25<sup>+</sup>FoxP3<sup>+</sup> cells.

Next, we compared the  $T_{\text{reg}}/T_{\text{conv}}$  ratio of  $\text{STAT5}^{\text{phospho}}$  levels between PFE and methanol-based permeabilization and found no significant differences (Figure 4E).

Finally, we investigated whether the alteration of CD25 and FoxP3 staining with PFE could be reproduced with different antibodies than CD25-PerCP-Cy5.5 and FoxP3-PE that were used here above. As shown in Supplemental Figure 4, CD25-PE showed satisfactory staining in comparison to the PFA condition while FoxP3-APC staining was completely lost. These results demonstrate that, for optimal results, the deleterious impact of PFE on specific antibodies should be evaluated before performing any analysis.

Altogether these data validate a 7-color staining method allowing measurement of  $\text{STAT5}^{\text{phospho}}$  levels together with Ki67 expression in mouse T-cell samples.

### In mouse splenocytes, naive $T_{\text{regs}}$ have higher $\text{STAT5}^{\text{phospho}}$ levels than effector $T_{\text{regs}}$ after stimulation with IL-2

Because IL-2 and  $\text{STAT5}^{\text{phospho}}$  play a major role in mouse  $T_{\text{reg}}$  homeostasis [29], we compared the  $\text{STAT5}^{\text{phospho}}$  response curve of naive and effector mouse  $T_{\text{regs}}$  to various concentrations of IL-2 (Figure 5A) by

using the following antibodies: CD4-eFluor450, CD25-PE-Cy7, CD62L-APC-eFluor780, CD44-FITC, CD103-BV510, FoxP3-PE, Ki67-PerCP-Cy5.5 and <sup>phospho</sup>STAT5-AlexaFluor647 (detailed in material and methods). In contrast to what was observed in human T<sub>regs</sub>, murine naive T<sub>regs</sub> responded to lower concentrations of IL-2 than effector T<sub>reg</sub> (Figure 5B). This is illustrated by the

significant difference of log(EC<sub>50</sub>) between the two subsets (naive T<sub>regs</sub>: 1.022 +/- 0.105 vs effector T<sub>regs</sub>: 1.416 +/- 0.088 (*p* = 0.0078)). This is consistent with a previous report showing that IL-2 injections in mice stimulated to a higher extent the proliferation of CD44<sup>low</sup>CD62L<sup>high</sup>CCR7<sup>+</sup> than CD44<sup>high</sup>CD62L<sup>low</sup>CCR7<sup>-</sup> T<sub>regs</sub> [30, 31]. Further, we investigated the respective expression of CD25 in both

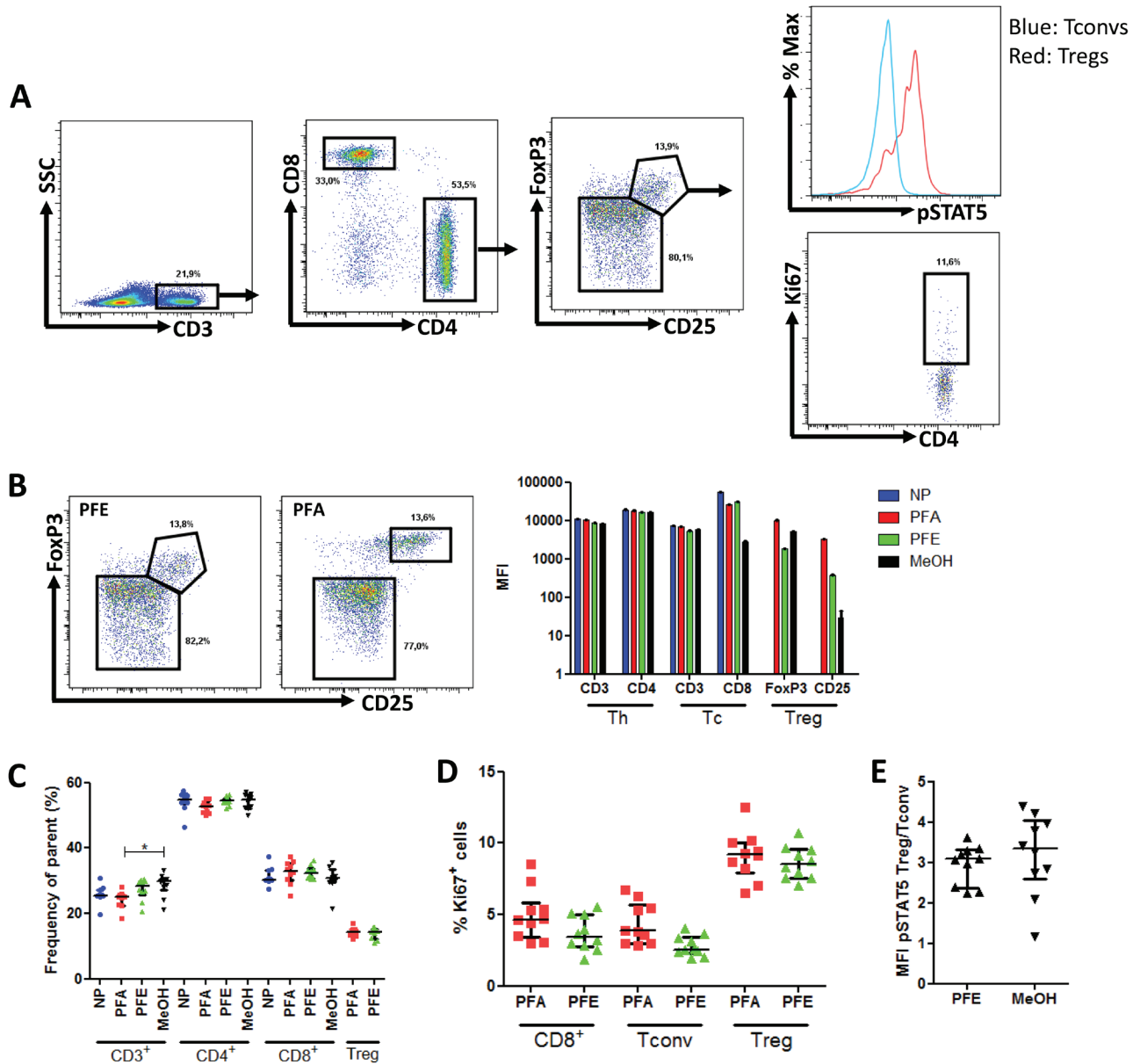


**Figure 4: Phospho-STAT5 analyzes in murine samples.** Splenocytes from 10 mice were surface stained with anti-CD3, -CD4, -CD8 and -CD25 antibodies and were either non permeabilized (NP) or stained with anti-FoxP3, -Ki67 and -<sup>phospho</sup>STAT5 antibodies after permeabilization with either paraformaldehyde (PFA)-based technique, PerFix EXPOSE (PFE) or methanol (MeOH)-based technique. Data show median values of 10 biological replicates / condition with interquartile range (\* *p* < 0.05, \*\**p* < 0.005, \*\*\**p* < 0.0005). **A.** Gating strategy of tubes permeabilized with the PFE technique. **B.** Impact of PerFix permeabilization on CD25 and FoxP3 staining (left panel) and on staining of markers of helper (Th), cytotoxic (Tc) and regulatory (T<sub>reg</sub>) T cells (right panel). **C.** Comparison of cell frequencies between the different permeabilization techniques: CD3<sup>+</sup> T cells among total splenocytes, CD4<sup>+</sup> helper and CD8<sup>+</sup> cytotoxic cells among CD3<sup>+</sup> T cells and CD25<sup>high</sup>FoxP3<sup>+</sup> among CD4<sup>+</sup> T cell. **D.** Comparison of Ki67<sup>+</sup> cell frequency within CD8<sup>+</sup> T cells, T<sub>conv</sub> and T<sub>regs</sub> between the PFA-based and PFE techniques. **E.** Comparison of ratio, for each sample, of <sup>phospho</sup>STAT5 MFI of T<sub>regs</sub> versus <sup>phospho</sup>STAT5 MFI of T<sub>conv</sub> in PerFix and methanol-based methods.

subsets and found that naive  $T_{reg}$  expressed higher levels of CD25 than effector  $T_{reg}$  in agreement with their response curves to IL-2 (Figure 5C) and with recently reported data [31]. As observed in human samples and taking data from  $T_{conv}$  and  $T_{reg}$  subsets together, there was a strong correlation between  $phospho$  STAT5 and CD25 levels (Spearman  $r = 0.82$ ,  $p < 0.0001$ , Figure 5D). However we found that activated  $T_{reg}$  expressed dramatically higher levels of Ki67 than naive  $T_{reg}$  (Figure 5E) and an inverse correlation between  $phospho$  STAT5 level and Ki67 was observed when taking data from  $T_{reg}$  subsets together (Spearman  $r = -0.75$ ,  $p < 0.0001$ , Figure 5F). Because the time of exposure to IL-2 in our experiments (15 min) is insufficient to induce Ki67 expression through the  $phospho$  STAT5 pathway (similar frequencies of Ki67 were found between stimulated and unstimulated  $T_{reg}$ , data not showed), these data suggest that  $T_{reg}$  proliferation is

conditioned by their activation status while their capacity to respond to IL-2 is conditioned by their expression of CD25.

In summary, we have validated a multicolor staining method that allows the measurement of STAT5 phosphorylation levels in human and murine  $T_{reg}$  subsets. Further, comparison of  $phospho$  STAT5 levels in response to IL-2 between the different  $T_{reg}$  subsets highlighted a striking divergence between the two species. These observations are in line with recent reports showing higher CD25 expression in activated effector  $T_{reg}$  than in naive  $T_{reg}$  in human PMBCs [8], but higher CD25 expression in naive  $T_{reg}$  than in effector  $T_{reg}$  in mouse splenocytes [31]. Further, as IL-2 administration has been previously shown to increase naive  $T_{reg}$  frequency in mouse [31] and activated ICOS<sup>+</sup>  $T_{reg}$  in humans [25], our work suggest that *ex vivo* response curves to cytokines might be predictive

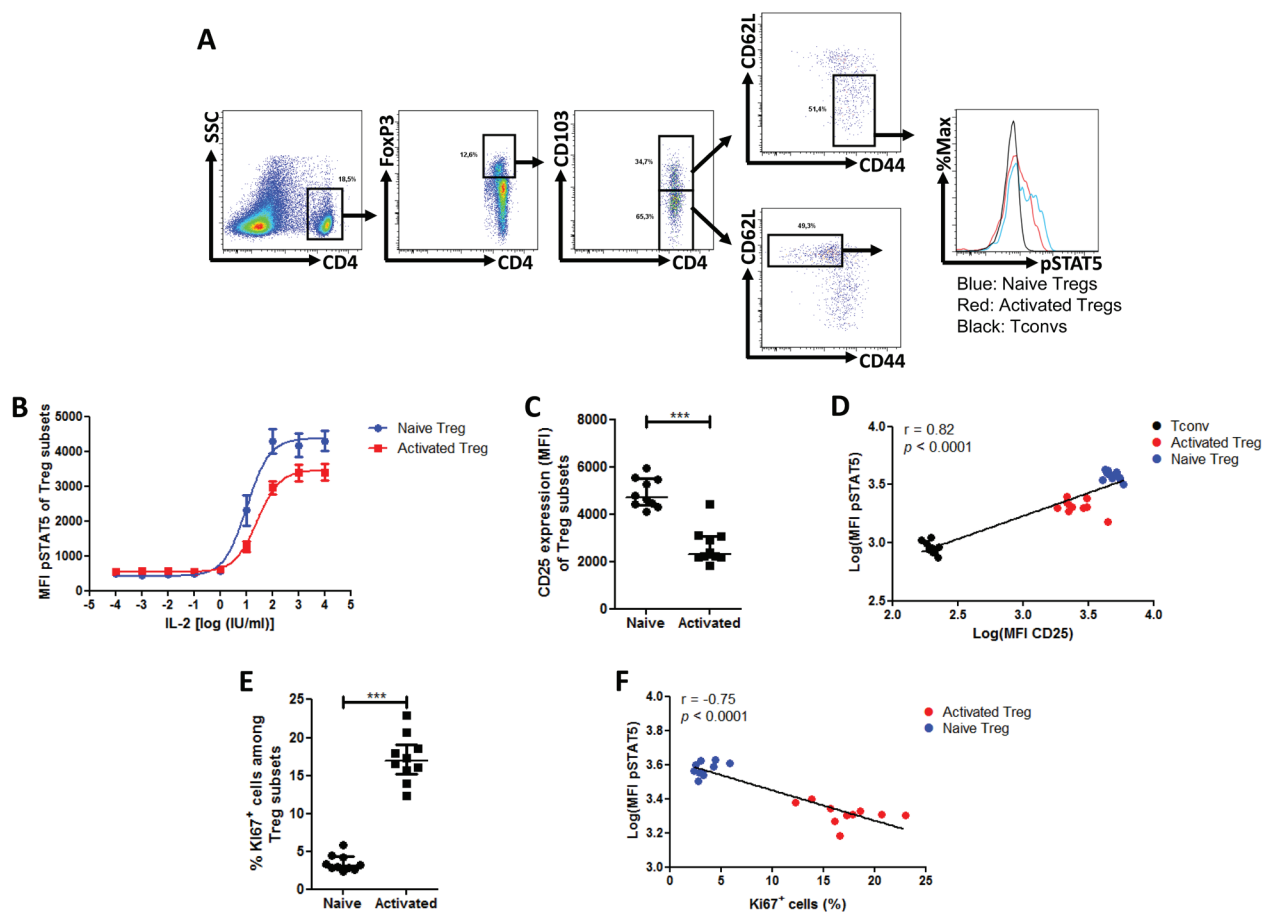


**Figure 5: Phospho-STAT5 comparison between murine  $T_{reg}$  subsets.** Mouse splenocytes were isolated from 10 animals, stimulated with 10 IU/ml IL-2, stained with anti-CD4, -CD25, -CD103, -CD62L, -CD44 surface antibodies, permeabilized with the PerFix EXPOSE method and stained with anti-FoxP3, -Ki67 and - $phospho$  STAT5 antibodies. Data show median values of 10 biological replicates / condition with interquartile range (\*  $p < 0.05$ , \*\*  $p < 0.005$ , \*\*\*  $p < 0.0005$ ). **A.** Gating strategy used to compare the naive ( $CD4^{+}FoxP3^{+}CD44^{low}CD62L^{high}CD103^{-}$ ) and activated ( $CD4^{+}FoxP3^{+}CD44^{high}CD62L^{low}CD103^{+}$ )  $T_{reg}$  subsets. **B.** Splenocytes were isolated from 3 B10.D2 mice, stimulated with various concentrations of IL-2 for 15 min and  $phospho$  STAT5 level was measured in  $T_{reg}$  subsets after PFE permeabilization. **C.** Comparison of CD25 expression (MFI) between the different  $T_{reg}$  subsets. **D.** Correlation between STAT5 phosphorylation level (log of MFI) and CD25 expression (log of MFI) in  $T_{conv}$  and the different  $T_{reg}$  subsets after stimulation with 10 IU/ml of IL-2. **E.** Comparison of Ki67<sup>+</sup> cell frequency among the different  $T_{reg}$  subsets. **F.** Correlation between STAT5 phosphorylation level (log of MFI) and Ki67<sup>+</sup> cell frequency in the different  $T_{reg}$  subsets after stimulation with 10 IU/ml of IL-2.



of the impact of specific cytokine administration on the homeostasis  $T_{reg}$  and other T-cell population.

## MATERIALS AND METHODS

### Volunteers

Blood from healthy adult volunteers (aged 21 to 37 years) was collected following written informed consent (approved by our local Ethic Committee). Peripheral blood mononuclear cells (PBMCs) were immediately isolated by density gradient centrifugation (Ficoll-Paque™, GE Healthcare, Upsala, Sweden) and then resuspended in staining buffer PBS+3%FBS (Lonza, Verviers, Belgium) at a concentration of  $1 \times 10^6$ /ml.

### Animal experiments

For the study assessing the impact of immunosuppressive drugs on human cells *in vivo*, NOD-scid IL-2R $\gamma^{null}$  (NSG) (The Jackson laboratory, Bar Harbor, ME) mice, aged from 8 to 9 weeks, were irradiated (2.5 Gy total body irradiation) and transplanted *i.v.* 24h later with  $5 \times 10^6$  human PBMCs (freshly isolated from one healthy volunteer). Animal weight and survival were monitored daily, in agreement with the recommendation of our ethical committee. Mice were then injected intraperitoneally with either PBS daily on days 4, 5 and 6 post-transplantation, 15 mg/kg of cyclosporin A (CSA, Sandimmune, Novartis, Basel, Switzerland) daily on days 4, 5 and 6 post-transplantation, 10 mg/kg of ATG (ATG-Fresenius, Neovii Biotech GmbH, Gräfelfing, Germany) on day 6 post-transplantation, or 50.000 IU of IL-2 (Proleukin, Novartis), 25h, 15h and 1h before the sacrifice at day 7.

For murine  $T_{reg}$  and phospho-STAT5 analyses, mice of either the B10.BR or B10.D2 strains (aged from 8-10 weeks) were sacrificed according to the local ethics policies without receiving any particular treatment. Splens of either NSG, B10.BR or B10.D2 mice were collected in RPMI supplemented with 5% FBS and were prepared to a single cell suspension. Cells were washed twice in staining buffer, filtered through a 75  $\mu$ m nylon mesh to remove aggregates, and were resuspended at a concentration of  $1 \times 10^6$  cells/ml in staining buffer.

### Cell culture and suppression assays

For *in vitro* drugs assays, freshly isolated human PBMCs from 3 healthy volunteers were activated in triplicate in the presence of anti-CD3/CD28 beads (Bead-Cell ratio 1:1, Invitrogen, Waltham, MA) in complete medium that consisted of RPMI 1640 L-glutamine

(2mM) (Lonza) supplemented with penicillin (100 IU/ml) (Lonza), streptomycin (10 mg/ml) (Lonza) and 10% human AB serum (Sigma-Aldrich, St. Louis, MO). Culture medium was supplemented with either PBS, 500 ng/ml of CSA, or 100  $\mu$ g/ml of ATG Fresenius/Neovii. Cells were collected for flow cytometry analysis after 24h of incubation at 37°C, 5% CO<sub>2</sub>.

For suppression assays,  $T_{reg}$  subsets were isolated from human PBMCs by flow cytometry (FACS Aria III, Becton Dickinson (BD), Bedford, MA). Sorted naive  $T_{conv}$  were loaded with CFSE 5  $\mu$ M (Invitrogen) and used as responder cells. Assays were performed in complete medium in the presence of anti-CD3/CD28 beads (Bead-Cell ratio 1:8, Invitrogen). Sorted  $T_{reg}$  and responder cells were cultured in mixed lymphocyte reactions at different  $T_{reg}$ : $T_{resp}$  ratios for 72h before analysis by flow cytometry.

### IL-2 stimulation

Human PBMCs or murine splenocytes ( $1 \times 10^6$  cells/ml in staining buffer) were stimulated with human recombinant IL-2 (Peprotech EC Ltd., London, UK) because recombinant human IL-2 has been proven to be also efficient in mouse [32, 33]. For all experiments other than dose-response curves, a concentration of 10 IU/ml was used, while for dose-response curve experiments, an 8-log range of concentrations was used for human and a 9-log range was used for murine experiments. Samples were stimulated for 15 min at 37°C and were immediately washed twice with staining buffer before processing for flow cytometry staining. This time of exposure was chosen based on phospho-STAT5 levels observed in lymphocytes after different times of stimulation with 10 IU/ml (Supplemental Figure 5), 15 min corresponding to a time point of maximal response.

### Flow cytometry

The following antibodies specific for human epitopes were used: CD4-PE-Cy5 (RPA-T4), CD25-BV421 (M-A251, BD), CD127-biotin (eBioRDR5), CD45RA-BV510 (HI100, BD), HLA-DR-APC-efluor780 (LN3), FOXP3-AlexaFluor488 (259D, Biolegend, ImTech Antwerp, Belgium), phosphoSTAT5-AlexaFluor647 (p7694, BD), Ki67-FITC (B56, BD), Ki67-PerCP-Cy5.5 (B56, BD), Ki67-PE (B56, BD) and anti-streptavidin-PE-Cy7. The following antibodies specific for mouse epitopes were used: CD3-V500 (500A2, BD), CD4-eFluor450 (RM4-5), CD8-PE-Cy7 (53-6.7), CD25-PerCP-Cy5.5 (PC61.5), CD25-PE-Cy7 (PC61, BD), CD25-PE (PC61.5), CD103-BV510 (M290, BD), CD44-FITC (IM7), CD62L-APC-eFluor780 (MEL-14), FoxP3-APC (FJK-16s), and FoxP3-PE (FJK-16s) (all from eBioscience, unless indicated otherwise). Cells ( $1 \times 10^6$  cells/sample) were incubated with surface antibodies for

20 min at 4°C in the dark and washed with staining buffer. This process was repeated for a 15-minute period for the streptavidin staining step. Then, samples were either not permeabilized and kept in PBS at 4°C until analysis by flow cytometry (Non Permeabilized (NP) condition) or were permeabilized by the use of one of three different procedures: the paraformaldehyde (PFA)-based method with FOXP3 Staining Buffer Set (eBioscience); the methanol (MeOH)-based method with Lyse/Fix buffer (Becton Dickinson) followed by Phosflow Perm Buffer III (Becton Dickinson) (Methanol-based method) or the PerFix EXPOSE (PFE, Beckman Coulter, Brea, CA) method. Manufacturer instructions were followed for each procedure. Data were acquired on a FACS Canto II (Becton Dickinson) and were analyzed with FlowJo v7.6.5 (Treestar Inc., San Carlos, CA).

### Gating strategy and definition of $T_{reg}$ subsets

In human samples,  $T_{regs}$  were defined as  $CD4^+CD25^+CD127^{dim}FOXP3^+$  lymphocytes. Naive  $T_{regs}$  were defined as  $CD45RA^+HLA-DR^{neg} T_{regs}$ , activated effector  $T_{regs}$  were defined as  $CD45RA^{neg}HLA-DR^+$   $T_{regs}$ , while HLA-DR<sup>neg</sup> effector  $T_{regs}$  were defined as  $CD45RA^{neg}HLA-DR^{neg} T_{regs}$  as recently proposed by Dong *et al.* [9]. In murine samples,  $T_{regs}$  were defined as  $CD4^+CD25^+FoxP3^+$  lymphocytes. Naive  $T_{regs}$  were defined as  $CD4^+FoxP3^+CD44^{low}CD62L^{high}CD103^-$  lymphocytes while effector  $T_{regs}$  were defined as  $CD4^+FoxP3^+CD44^{high}CD62L^{low}CD103^+$  lymphocytes [4].

### Statistical analyses

The Mann-Whitney *U* test was used to compare flow cytometry data from different treatments. The extra sum-of-squares *F* test was used to compare the half maximal effective concentrations ( $EC_{50}$ ). The Spearman test was used to assess correlations. Statistical analyses were carried out with Graphpad Prism 5.0 (Graphpad Software, San Diego, CA). *P* values < 0.05 were considered as statistically significant.

### ACKNOWLEDGMENTS

We are very grateful to Sandra Ormenese from the Imaging and Flow Cytometry Platform of the GIGA for help with flow cytometers.

### GRANT SUPPORT

This study was supported by funds from: the National Fund for Scientific Research (FNRS), the Leon Fredericq fund and Anti-Cancer Center at the University of Liège, and the Belgian Federation Against Cancer. GE is Télévie Research Assistant, and FB is senior

research associate of the National Fund for Scientific Research (FNRS) Belgium. SHB is funded by the Fonds Wetenschappelijk Onderzoek (FWO).

### CONFLICTS OF INTEREST

The authors declare no conflicts of interest.

### Authors' contributions

Study design: GE, FB, SHB; Data acquisition: GE, MH; Data interpretation: GE, MH, SHB; Ms writing GE, FB; Manuscript editing MH, YB, SHB; Approval of the last version of the manuscript: all authors.

### REFERENCES

1. Sakaguchi S, Sakaguchi N, Asano M, Itoh M and Toda M. Immunologic self-tolerance maintained by activated T cells expressing IL-2 receptor alpha-chains (CD25). Breakdown of a single mechanism of self-tolerance causes various autoimmune diseases. *Journal of Immunology*. 1995; 155:1151-1164.
2. Tian L, Humblet-Baron S and Liston A. Immune tolerance: are regulatory T cell subsets needed to explain suppression of autoimmunity? *Bioessays*. 2012; 34:569-575.
3. Josefowicz SZ, Lu LF and Rudensky AY. Regulatory T cells: mechanisms of differentiation and function. *Annu Rev Immunol*. 2012; 30:531-564.
4. Liston A and Gray DH. Homeostatic control of regulatory T cell diversity. *Nature reviews Immunology*. 2014; 14:154-165.
5. Seddiki N, Santner-Nanan B, Martinson J, Zaunders J, Sasson S, Landay A, Solomon M, Selby W, Alexander SI, Nanan R, Kelleher A and Fazekas de St Groth B. Expression of interleukin (IL)-2 and IL-7 receptors discriminates between human regulatory and activated T cells. *The Journal of experimental medicine*. 2006; 203:1693-1700.
6. Abbas AK, Benoist C, Bluestone JA, Campbell DJ, Ghosh S, Hori S, Jiang S, Kuchroo VK, Mathis D, Roncarolo MG, Rudensky A, Sakaguchi S, Shevach EM, et al. Regulatory T cells: recommendations to simplify the nomenclature. *Nat Immunol*. 2013; 14:307-308.
7. Gratz IK and Campbell DJ. Organ-specific and memory treg cells: specificity, development, function, and maintenance. *Frontiers in immunology*. 2014; 5:333.
8. Miyara M, Yoshioka Y, Kitoh A, Shima T, Wing K, Niwa A, Parizot C, Taffin C, Heike T, Valeyre D, Mathian A, Nakahata T, Yamaguchi T, Nomura T, Ono M, Amoura Z, et al. Functional delineation and differentiation dynamics of human CD4<sup>+</sup> T cells expressing the FoxP3 transcription factor. *Immunity*. 2009; 30:899-911.
9. Dong S, Maiella S, Xhaard A, Pang Y, Wenandy L, Larghero J, Becavin C, Benecke A, Bianchi E, Socie G and

- Rogge L. Multiparameter single-cell profiling of human CD4+FOXP3+ regulatory T-cell populations in homeostatic conditions and during graft-*versus*-host disease. *Blood*. 2013; 122:1802-1812.
10. Miyara M, Ito Y and Sakaguchi S. TREG-cell therapies for autoimmune rheumatic diseases. *Nature reviews Rheumatology*. 2014; 10:543-551.
  11. Socie G and Ritz J. Current issues in chronic graft-*versus*-host disease. *Blood*. 2014; 124:374-84.
  12. Edinger M, Hoffmann P, Ermann J, Drago K, Fathman CG, Strober S, Negrin RS. CD4+CD25+ regulatory T cells preserve graft-*versus*-tumor activity while inhibiting graft-*versus*-host disease after bone marrow transplantation. *Nat Med*. 2003; 9:1144-50.
  13. Cohen JL, Trenado A, Vasey D, Klatzmann D and Salomon BL. CD4(+)CD25(+) immunoregulatory T Cells: new therapeutics for graft-*versus*-host disease. *Journal of Experimental Medicine*. 2002; 196:401-406.
  14. Hannon M, Lechanteur C, Lucas S, Somja J, Seidel L, Belle L, Bruck F, Baudoux E, Giet O, Chantillon AM, Delvenne P, Drion P, Beguin Y, et al. Infusion of clinical-grade enriched regulatory T cells delays experimental xenogeneic graft-*versus*-host disease. *Transfusion*. 2014; 54:353-363.
  15. Hippen KL, Merkel SC, Schirm DK, Sieben CM, Sumstad D, Kadidlo DM, McKenna DH, Bromberg JS, Levine BL, Riley JL, June CH, Scheinberg P, Douek DC, et al. Massive ex vivo expansion of human natural regulatory T cells (T(regs)) with minimal loss of *in vivo* functional activity. *SciTranslMed*. 2011; 3:83ra41.
  16. Sagoo P, Ali N, Garg G, Nestle FO, Lechler RI and Lombardi G. Human regulatory T cells with alloantigen specificity are more potent inhibitors of alloimmune skin graft damage than polyclonal regulatory T cells. *Science translational medicine*. 2011; 3:83ra42.
  17. Di Ianni M, Falzetti F, Carotti A, Terenzi A, Castellino F, Bonifacio E, Del Papa B, Zei T, Ostini RI, Cecchini D, Aloisi T, Perruccio K, Ruggeri L, Balucani C, Pierini A, Sportoletti P, et al. Tregs prevent GVHD and promote immune reconstitution in HLA-haploidentical transplantation. *Blood*. 2011; 117:3921-3928.
  18. Brunstein CG, Miller JS, Cao Q, McKenna DH, Hippen KL, Curtsinger J, DeFor T, Levine BL, June CH, Rubinstein P, McGlave PB, Blazar BR and Wagner JE. Infusion of ex vivo expanded T regulatory cells in adults transplanted with umbilical cord blood: safety profile and detection kinetics. *Blood*. 2011; 117:1061-1070.
  19. Theil A, Tuve S, Oelschlagel U, Maiwald A, Dohler D, Ossmann D, Zenkel A, Wilhelm C, Middeke JM, Shayegi N, Trautmann-Grill K, von Bonin M, Platzbecker U, et al. Adoptive transfer of allogeneic regulatory T cells into patients with chronic graft-*versus*-host disease. *Cytotherapy*. 2015; 17:473-86.
  20. van der Net JB, Bushell A, Wood KJ and Harden PN. Regulatory T cells: first steps of clinical application in solid organ transplantation. *Transplant international*. 2015 May 15. [Epub ahead of print] PMID:25981203.
  21. Boyman O and Sprent J. The role of interleukin-2 during homeostasis and activation of the immune system. *Nature reviews Immunology*. 2012; 12:180-190.
  22. Koreth J, Matsuoka K, Kim HT, McDonough SM, Bindra B, Alyea EP, III, Armand P, Cutler C, Ho VT, Treister NS, Bienfang DC, Prasad S, Tzachanis D, Joyce RM, Avigan DE, Antin JH, et al. Interleukin-2 and regulatory T cells in graft-*versus*-host disease. *New England Journal of Medicine*. 2011; 365:2055-2066.
  23. Saadoun D, Rosenzweig M, Joly F, Six A, Carrat F, Thibault V, Sene D, Cacoub P and Klatzmann D. Regulatory T-cell responses to low-dose interleukin-2 in HCV-induced vasculitis. *The New England journal of medicine*. 2011; 365:2067-2077.
  24. Rosenzweig M, Churlaud G, Mallone R, Six A, Derian N, Chaara W, Lorenzon R, Long SA, Buckner JH, Afonso G, Pham HP, Hartemann A, Yu A, et al. Low-dose interleukin-2 fosters a dose-dependent regulatory T cell tuned milieu in T1D patients. *J Autoimmun*. 2015; 58:48-58.
  25. Sim GC, Martin-Orozco N, Jin L, Yang Y, Wu S, Washington E, Sanders D, Lacey C, Wang Y, Vence L, Hwu P and Radvanyi L. IL-2 therapy promotes suppressive ICOS+ Treg expansion in melanoma patients. *J Clin Invest*. 2014; 124:99-110.
  26. Baron F, Labopin M, Blaise D, Lopez-Corral L, Vigouroux S, Craddock C, Attal M, Jindra P, Goker H, Socie G, Chevallier P, Browne P, Sandstedt A, et al. Impact of *in vivo* T-cell depletion on outcome of AML patients in first CR given peripheral blood stem cells and reduced-intensity conditioning allo-SCT from a HLA-identical sibling donor: a report from the Acute Leukemia Working Party of the European Group for Blood and Marrow Transplantation. *Bone marrow transplantation*. 2014; 49:389-396.
  27. Feng X, Kajigaya S, Solomou EE, Keyvanfar K, Xu X, Raghavachari N, Munson PJ, Herndon TM, Chen J and Young NS. Rabbit ATG but not horse ATG promotes expansion of functional CD4+CD25highFOXP3+ regulatory T cells *in vitro*. *Blood*. 2008; 111:3675-3683.
  28. Shimony O, Nagler A, Gellman YN, Refaeli E, Rosenblum N, Eshkar-Sebban L, Yerushalmi R, Shimoni A, Lytton SD, Stanevsky A, Or R and Naor D. Anti-T lymphocyte globulin (ATG) induces generation of regulatory T cells, at least part of them express activated CD44. *J Clin Immunol*. 2012; 32:173-188.
  29. Pierson W, Cauwe B, Policheni A, Schlenner SM, Franckaert D, Berges J, Humblet-Baron S, Schonefeldt S, Herold MJ, Hildeman D, Strasser A, Bouillet P, Lu LF, Matthys P, Freitas AA, Luther RJ, et al. Antiapoptotic Mcl-1 is critical for the survival and niche-filling capacity of Foxp3(+) regulatory T cells. *Nature Immunology*. 2013; 14:959-965.
  30. Smigielski KS, Srivastava S, Stolley JM and Campbell DJ.

Regulatory T-cell homeostasis: steady-state maintenance and modulation during inflammation. *Immunol Rev.* 2014; 259:40-59.

31. Smigiel KS, Richards E, Srivastava S, Thomas KR, Dudda JC, Klonowski KD and Campbell DJ. CCR7 provides localized access to IL-2 and defines homeostatically distinct regulatory T cell subsets. *The Journal of experimental medicine.* 2014; 211:121-136.
32. Rosenberg SA, Lotze MT, Muul LM, Leitman S, Chang AE, Ettinghausen SE, Matory YL, Skibber JM, Shiloni E, Vetto JT, Scipp CA, Simpson C and Reichert CM. Observation on the systemic administration of autologous lymphokine-activated killer cells and recombinant interleukin-2 to patients with metastatic cancer. *New England Journal of Medicine.* 1985; 313:1485-1492.
33. Tang Q, Adams JY, Penaranda C, Melli K, Piaggio E, Sgouroudis E, Piccirillo CA, Salomon BL and Bluestone JA. Central role of defective interleukin-2 production in the triggering of islet autoimmune destruction. *Immunity.* 2008; 28:687-697.